Neural deficits contribute to respiratory insufficiency in Pompe disease

Lara R. DeRuisseau[a], David D. Fuller[b], Kai Qiu[b], Keith C. DeRuisseau[c], William H. Donnelly, Jr.[d], Cathryn Mah[e], Paul J. Reier[f], and Barry J. Byrne[g,1]

[a]Department of Physiological Sciences, College of Veterinary Medicine, [b]Department of Physical Therapy, College of Public Health and Health Professions, [c]Department of Applied Physiology and Kinesiology, College of Health and Human Performance; and Departments of [d]Pathology, [e]Cellular and Molecular Therapy, [f]Neuroscience, and [g]Pediatrics, Molecular Genetics, and Microbiology and Powell Gene Therapy Center, College of Medicine, University of Florida, Gainesville, FL 32610

Communicated by Kenneth I. Berns, University of Florida College of Medicine, Gainesville, FL, April 9, 2009 (received for review February 1, 2008)

Pompe disease is a severe form of muscular dystrophy due to glycogen accumulation in all tissues, especially striated muscle. Disease severity is directly related to the deficiency of acid α-glucosidase (GAA), which degrades glycogen in the lysosome. Respiratory dysfunction is a hallmark of the disease, muscle weakness has been viewed as the underlying cause, and the possibility of an associated neural contribution has not been evaluated previously. Therefore, we examined behavioral and neurophysiological aspects of breathing in 2 animal models of Pompe disease—the *Gaa*$^{-/-}$ mouse and a transgenic line (MTP) expressing GAA only in skeletal muscle, as well as a detailed analysis of the CNS in a Pompe disease patient. Glycogen content was elevated in the *Gaa*$^{-/-}$ mouse cervical spinal cord. Retrograde labeling of phrenic motoneurons showed significantly greater soma size in *Gaa*$^{-/-}$ mice vs. isogenic controls, and glycogen was observed in *Gaa*$^{-/-}$ phrenic motoneurons. Ventilation, assessed via plethysmography, was attenuated during quiet breathing and hypercapnic challenge in *Gaa*$^{-/-}$ mice (6 to >21 months of age) vs. controls. We confirmed that MTP mice had normal diaphragmatic contractile properties; however, MTP mice had ventilation similar to the *Gaa*$^{-/-}$ mice during quiet breathing. Neurophysiological recordings indicated that efferent phrenic nerve inspiratory burst amplitudes were substantially lower in *Gaa*$^{-/-}$ and MTP mice vs. controls. In human samples, we demonstrated similar pathology in the cervical spinal cord and greater accumulation of glycogen in spinal cord compared with brain. We conclude that neural output to the diaphragm is deficient in *Gaa*$^{-/-}$ mice, and therapies targeting muscle alone may be ineffective in Pompe disease.

glycogenosis | motor neuron | muscular dystrophy | myopathy

Glycogen is normally absent from neurons (1), and glycogen accumulation is associated with apoptosis in neural cell cultures (2). Accumulation of neuronal glycogen may be particularly relevant with respect to glycogen storage diseases (3). For example, Pompe disease is both a lysosomal and glycogen storage disorder resulting from a recessively inherited deficiency of acid α-glucosidase (GAA) (reviewed in ref. 4). GAA is normally active in the lysosome, where it degrades excess glycogen by cleaving the α-1,4 glycosidic bonds (5) and α-1,6 glycosidic bonds (6). Without adequate GAA activity, glycogen accumulates in muscle cells and neurons (3, 4).

Complete GAA deficiency occurs in approximately 1 of every 40,000 infants, with a prevalence of several thousand patients worldwide (4, 7, 8). In these Pompe infants, respiratory muscle weakness contributes substantially to morbidity, and cardiorespiratory failure usually occurs by 8–10 months of age. Juvenile and adult forms of the disease show reduced but residual GAA activity and a slower progression of symptoms (4, 8). Cardiac involvement is mild in these later-onset patients, and respiratory insufficiency often leads to ventilator dependency and, ultimately, respiratory failure (4).

Although it is generally accepted that diaphragmatic dysfunction is the primary reason for ventilation deficits in Pompe disease, there has been no formal effort to explore a potential neural contribution to the respiratory-related pathophysiology of this disease. However, a few Pompe case reports have demonstrated CNS glycogen accumulation (9–14) and absent or diminished deep tendon reflexes (15, 16). In particular, spinal motoneurons seem to be susceptible to excessive glycogen accumulation (10, 13, 15). The large, swollen appearance of these cells (10, 12) suggests possible neurophysiological implications, such as altered excitability. Accordingly, we postulated that GAA deficiency in the nervous system may contribute to respiratory insufficiency and tested the hypothesis that GAA-deficient mice (*Gaa*$^{-/-}$) would exhibit reduced ventilation, and this would be reflected by attenuated efferent phrenic motor discharge. Testing this hypothesis raises important considerations for the approach to Pompe disease therapy because the only currently available strategy, enzyme replacement therapy, does not effectively target GAA deficiency and glycogen accumulation in the CNS (17, 18).

Results

Body Weight. *Gaa*$^{-/-}$ mice weighed less than wild-type controls at all ages, and *Gaa*$^{-/-}$ males weighed more than females at all ages (Table S1).

Cervical Spinal Glycogen Quantification and Histology. Cervical spinal cord (C_3–C_5) glycogen contents (micrograms per milligram of wet weight) were 11 ± 1, 15 ± 2, and 17 ± 1 in wild-type control mice at ages 6, 12, and >21 months, respectively. In contrast, *Gaa*$^{-/-}$ mice at 6, 12, and >21 months had values of 21 ± 1, 28 ± 1, and 38 ± 2, respectively (all $P < 0.01$ vs. control). These data were confirmed in independent experiments where glycogen was quantified at multiple levels of the spinal neuraxis (Fig. S1).

Correlative histochemistry demonstrated significant glycogen reaction product in *Gaa*$^{-/-}$ mouse neuronal cell bodies throughout the gray matter of the cervical spinal cord that was especially prominent in motoneurons (Fig. 1). Motoneurons in the *Gaa*$^{-/-}$ ventral cervical spinal cord retrogradely labeled with fluorogold exhibited prominent periodic acid/Schiff (PAS) droplets (positive glycogen) throughout the cell body cytoplasm (Fig. 1 *B* and *F*–*H*). Comparable neurons from PAS-stained sections of control specimens showed neurons with virtually no PAS-positive inclusions (Fig. 1 *A* and *D*). Additional studies were conducted in which cholera toxin β-subunit (CT-β) was applied to the diaphragm to retrogradely label phrenic motoneurons. We observed fewer labeled phrenic motoneurons in *Gaa*$^{-/-}$ (148 ± 10) vs. control (220 ±

Author contributions: L.R.D., D.D.F., C.M., P.J.R., and B.J.B. designed research; L.R.D., D.D.F., K.Q., and K.C.D. performed research; L.R.D., D.D.F., K.Q., K.C.D., W.H.D., P.J.R., and B.J.B. contributed new reagents/analytic tools; L.R.D., D.D.F., K.Q., W.H.D., P.J.R., and B.J.B. analyzed data; and L.R.D., D.D.F., P.J.R., and B.J.B. wrote the paper.

Conflict of interest statement: B.J.B., The Johns Hopkins University, and the University of Florida could be entitled to patent royalties for inventions described in this manuscript.

[1]To whom correspondence should be addressed. E-mail: bbyrne@ufl.edu.

This article contains supporting information online at www.pnas.org/cgi/content/full/0902534106/DCSupplemental.

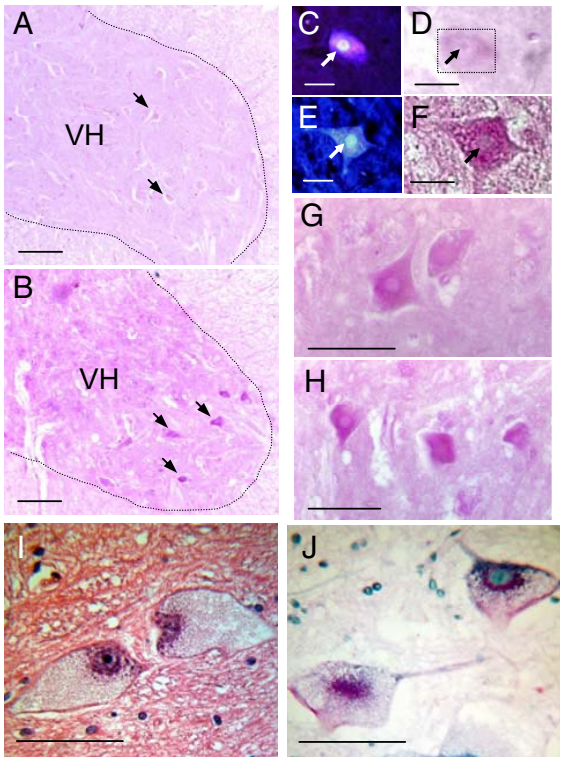

Fig. 1. Cervical spinal cord histology in B6/129 and *Gaa*$^{-/-}$ mice as well as a Pompe patient. (*A* and *B*) The C4 ventral horn (VH) of a control B6/129 mouse (*A*) and a *Gaa*$^{-/-}$ mouse (*B*). Arrows indicate neuronal cell bodies. Positive staining for glycogen reaction product (PAS stain; pink) was virtually absent in the control cord (*A*) compared with the *Gaa*$^{-/-}$ cord (*B*). Putative motoneuron cell bodies showed PAS reaction product in *Gaa*$^{-/-}$ spinal cords (e.g., arrows in *B*), and therefore additional experiments were conducted to retrogradely label phrenic motoneurons before PAS staining. (*C* and *D*) Fluorogold labeling (*C*) and PAS staining (*D*) of the same cell in a control mouse. The PAS stain is very light in this control tissue, and therefore the box in *D* outlines the same phrenic motoneuron fluorescently labeled in *C* (arrows point to nucleus). (*E* and *F*) Fluorogold (*E*) and PAS staining (*F*) in a *Gaa*$^{-/-}$ phrenic motoneuron. (*G* and *H*) Additional examples of PAS-positive neurons observed in the VH of the C4 spinal cord of *Gaa*$^{-/-}$ mice. Tissue was also obtained from the VH of the cervical spinal cord of a Pompe patient (see *Materials and Methods*) and stained with hematoxylin and eosin (*I*) and PAS (*J*). Pompe neurons in the ventral cervical horn had a swollen cell body with a nucleus located in an eccentric position within the cell soma (*I*). PAS staining indicates glycogen accumulation within the cell soma (*J*). (Scale bars: *A* and *B*, 100 μm; *C–F*, 20 μm; *G–J*, 50 μm.)

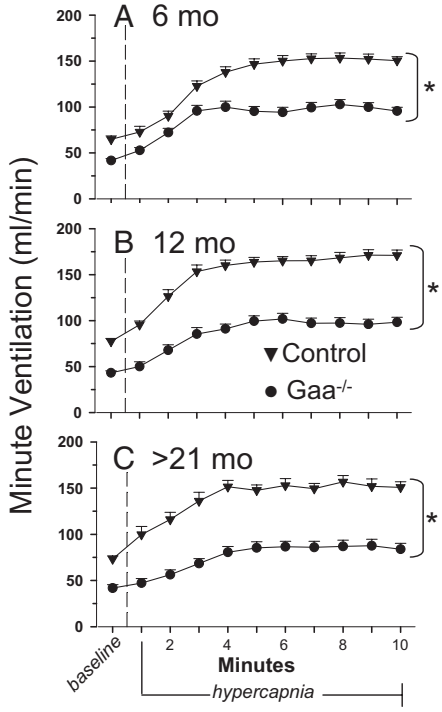

Fig. 2. Ventilation measured with whole-body plethysmography in B6/129 and *Gaa*$^{-/-}$mice. Minute ventilation (mLs per minute) was measured during quiet breathing (i.e., baseline, 21% O_2, balance N_2), followed by a 10-min hypercapnic challenge (7% CO_2, balance O_2). *A–C* Data from B6/129 control (▼) and *Gaa*$^{-/-}$ mice (●) of different ages: 6 months (*A*), 12 months (*B*), and >21 months (*C*). *, Control response is different from *Gaa*$^{-/-}$ response, $P < 0.01$.

22; $P = 0.015$) mice and, on average, phrenic motoneuron soma size was larger in *Gaa*$^{-/-}$ (812 ± 25 μm^2) vs. control mice (642 ± 28 μM^2 $P = 0.014$).

Ventilation. *Gaa*$^{-/-}$ mice appeared to be hypoventilating based on the minute ventilation to expired CO_2 ratio, which normalizes minute ventilation to metabolic CO_2 production. This measure was attenuated at baseline in *Gaa*$^{-/-}$ mice vs. wild-type controls (Fig. S2). Baseline minute ventilation, breathing frequency, tidal volume, peak inspiratory flow, peak expiratory flow, and tidal volume to inspiratory time ratio were also decreased in *Gaa*$^{-/-}$ mice compared with controls at all ages studied (Fig. 2 and Table 1). The only age differences detected were lower frequency at >21 months (vs. 6 months) and elevated tidal volume at >21 months (vs. 6 months). No strain by age interaction was detected.

Hypercapnic challenge was used as a respiratory stimulus to test the capacity to increase ventilation in *Gaa*$^{-/-}$ mice. Hypercapnic minute ventilation was lower for *Gaa*$^{-/-}$ mice vs. controls at all ages (Fig. 2). Additional ventilatory parameters were also attenuated, including frequency, tidal volume, peak inspiratory flow, peak expiratory flow, and the tidal volume to inspiratory time ratio (i.e., mean inspiratory airflow rate). Sex differences were only detected in the hypercapnic response of the 6-month age group (Table S2).

Blood Sampling. Both hemoglobin (Hb) and hematocrit (Hct) were elevated in *Gaa*$^{-/-}$ mice (Table 2), possibly reflecting a compensatory response to reduced arterial partial pressure of O_2 (P_aO_2; see below). In addition, glucose and sodium levels did not vary between groups, suggesting that the measured Hb and Hct differences did not reflect plasma volume differences. *Gaa*$^{-/-}$ mice had lower P_aO_2 vs. controls (Table 2), supporting the concept that these mice hypoventilate.

Muscle-Specific hGAA Mice. We next studied a group of transgenic animals with muscle-specific correction of GAA activity (MTP mice) (18). Male MTP mice ($n = 6$) were studied at a single age (12 months). MTP mouse body weight (40.6 ± 2.5 g) was similar to B6/129 but greater than *Gaa*$^{-/-}$ mice at similar ages (see Table S1). Spinal cord glycogen content was measured in MTP mice (26.9 ± 1.1 μg/mg wet weight, $n = 3$, age 18 months) and was similar to values obtained for *Gaa*$^{-/-}$ mice (28 ± 1 μg/mg wet weight). To first obtain an index of diaphragm muscle function, we measured in vitro contractile properties from B6/129, *Gaa*$^{-/-}$, and MTP mice. Control and MTP mice had similar diaphragm force generation, whereas the *Gaa*$^{-/-}$ diaphragm produced significantly smaller forces (Fig. 3*A*). These data confirm that the normal glycogen levels in MTP diaphragm muscle (MTP vs. B6/129, 1.7 ± 1.3 vs. 1.4 ± 0.2 μg/mg wet weight) correspond to diaphragm muscle that is functionally similar to the B6/129 control animals.

Despite apparently normal functional diaphragm muscle (Fig. 3*A*), the pattern of breathing was altered in the MTP mice. Minute

Table 1. Baseline ventilation characteristics

Group	Frequency, breaths per minute	TV, milliliters per breath	MV, mL/min	PIF, mL/sec	PEF, mL/sec	TV/T_i, mL/sec
6 months						
Control	239 ± 7	0.27 ± 0.00	64.8 ± 3.7	5.9 ± 0.2	3.4 ± 0.2	3.4 ± 0.2
Gaa$^{-/-}$	197 ± 6*	0.21 ± 0.00*	41.6 ± 2.3*	3.3 ± 0.2*	2.2 ± 0.1*	1.7 ± 0.1*
12 months						
Control	252 ± 7	0.31 ± 0.00	77.3 ± 3.4	6.7 ± 0.2	4.4 ± 0.2	3.9 ± 0.2
Gaa$^{-/-}$	186 ± 7*	0.23 ± 0.00*	43.2 ± 2.3*	3.6 ± 0.1*	2.3 ± 0.1*	2.1 ± 0.1*
>21 months						
Control	225 ± 7†	0.33 ± 0.00†	73.4 ± 3.2	6.3 ± 0.3	4.6 ± 0.2	3.7 ± 0.2
Gaa$^{-/-}$	168 ± 7*†	0.25 ± 0.01*†	41.8 ± 3.8*	3.5 ± 0.3*	2.3 ± 0.2*	2.1 ± 0.2*

Baseline (21% O_2, balanced N_2) values for frequency, tidal volume (TV), minute ventilation (MV), peak inspiratory flow (PIF), peak expiratory flow (PEF), and tidal volume to inspiratory time ratio (TV/T_i) of control and *Gaa*$^{-/-}$ mice.
**Gaa*$^{-/-}$ different from control ($P < 0.01$).
†More than 21 months is different from 6 months ($P < 0.01$). See supplement for *n* values (Table S3).

ventilation during baseline, or quiet breathing, was similar in MTP and *Gaa*$^{-/-}$ mice, and both were significantly reduced compared with B6/129 mice (Fig. 3*B*). Furthermore, the response to hypercapnia was significantly attenuated in MTP mice, although they showed a greater response than the *Gaa*$^{-/-}$ mice (Fig. 3*B*). The MTP mice were derived by crossing *Gaa*$^{-/-}$ mice with the FVB strain. Accordingly, in additional experiments we confirmed that ventilation in both MTP and *Gaa*$^{-/-}$ mice was lower than FVB mice under comparable conditions. Specifically, ventilation was 34% and 30% lower (vs. FVB) in MTP and *Gaa*$^{-/-}$ mice, respectively. This difference reflected primarily a reduction in tidal volume.

Efferent Phrenic Activity. To determine whether the compromised ventilation seen in *Gaa*$^{-/-}$ and MTP was associated with reduced phrenic motor output, we measured efferent phrenic nerve activity in *Gaa*$^{-/-}$, MTP, and control mice. At similar arterial PCO_2 levels (see legend to Fig. 4*A*), *Gaa*$^{-/-}$ and MTP mice had significantly lower phrenic inspiratory burst amplitudes (Fig. 4*A*). *Gaa*$^{-/-}$ and MTP mice also had reduced phrenic burst frequency and an attenuated slope of the integrated inspiratory burst (i.e., slower "rate of rise"; Table 3).

Pompe Patient Data. A Pompe patient who suffered progressive ventilatory insufficiency died at 18 months of age. The patient had been treated with rhGAA since 6 months of age. We were able to obtain cervical spinal and brain tissue samples from this patient that were fixed or frozen rapidly at autopsy, and frozen samples were stored at −80 °C until assayed. Glycogen content was 4-fold higher in the spinal cord (0.04%) compared with brain tissue (0.01%). The spinal cord data were compared to values obtained from similar age porcine tissue because autopsy material for rapidly processed neural tissue is difficult to obtain. Glycogen was negligible in the porcine spinal cord (0.001%). In addition, histology samples obtained from the ventral horn of the cervical cord (C4) showed pathology as reflected by neurons with a swollen cell body and chromatolysis-like appearance in that the nucleus was located in an eccentric position within the cell soma (Fig. 1*I*). In addition, chromophilic substance is concentrated around the nucleus. The remainder of the cytoplasm had a granular appearance (Fig. 1*I*). PAS staining of the human spinal cord revealed glycogen-laden motor neurons (Fig. 1*J*), consistent with the findings in the animal model.

Table 2. Blood characteristics for 12-month *Gaa*$^{-/-}$ and control mice

Group	Hemoglobin, g/dL	Hematocrit, %	Sodium, mmol/L	Glucose, mg/dL	P_aO_2, mmHG
Control	13.5 ± 0.3	39.8 ± 0.9	144.5 ± 0.8	180.4 ± 16.3	98.5 ± 1.9
Gaa$^{-/-}$	15.3 ± 0.4*	45.0 ± 1.1*	143.4 ± 0.9	176.8 ± 11.4	83.3 ± 2.7*

Hemoglobin, hematocrit, sodium, and glucose values for control and *Gaa*$^{-/-}$ mice at 12 months of age ($n = 9$ per group). Arterial partial pressure of O_2 for control and *Gaa*$^{-/-}$ mice at 12 months of age ($n = 6$ per group).
**Gaa*$^{-/-}$ different from control ($P < 0.01$).

Discussion

This study of a murine model of Pompe disease has revealed several novel observations pertaining to GAA deficiency and concomitant respiratory involvement. First, ventilation is reduced in *Gaa*$^{-/-}$ mice, as revealed by plethysmography. Second, cervical spinal cord glycogen is elevated in *Gaa*$^{-/-}$ mice, and PAS staining identified prominent glycogen inclusions in cervical motoneurons, including phrenic motoneurons identified by retrograde tracing. Phrenic motoneurons also had larger soma area compared with wild-type controls. Similar histopathology was also observed in a Pompe patient sample of the cervical spinal cord. Third, *Gaa*$^{-/-}$ mice have attenuated phrenic output relative to wild-type controls. Lastly, MTP mice also exhibit breathing impairments and phrenic neurogram features similar to those observed in *Gaa*$^{-/-}$ mice, despite apparently normal diaphragmatic contractile function. To our knowledge, these are the first formal lines of evidence suggesting respiratory weakening in the *Gaa*$^{-/-}$ mouse, and by extrapolation in Pompe disease patients, are the result of a combination of both neural and muscular deficits.

The Gaa$^{-/-}$ Mouse Model and Altered Ventilation. Our findings demonstrate that *Gaa*$^{-/-}$ mice exhibit a ventilatory phenotype similar to juvenile- and adult-onset Pompe disease patients, although it is unclear why ventilation did not decline further with age. Nevertheless, the *Gaa*$^{-/-}$ mouse used in this investigation is presently the most compelling available model of this disorder. To date, studies have shown glycogen accumulation in virtually all tissues of the *Gaa*$^{-/-}$ mouse (3, 19), and physiological measures appear strikingly similar to what is seen in the patient population (3). Cardiac pathology in these mice is not as severe as in infants with Pompe disease (20), but instead more closely corresponds to juvenile- and adult-onset patients (4).

The *Gaa*$^{-/-}$ mouse line used in this study was developed from a chimera of B6 and 129 mouse strains (19). This diverse genetic background could result in different compensatory mechanisms depending on the genetic proportion of B6 and 129 in each individual *Gaa*$^{-/-}$ mouse. However, both B6 and 129 inbred mice demonstrate similar minute ventilation values at baseline and in response to hypercapnia (21). Furthermore, we have successfully maintained this line for more than 5 years with brother-to-sister matings to establish as homogeneous a background as possible. To circumvent any issues involving this background strain, we also tested large numbers of mice. In addition, we followed the guide-

MEDICAL SCIENCES

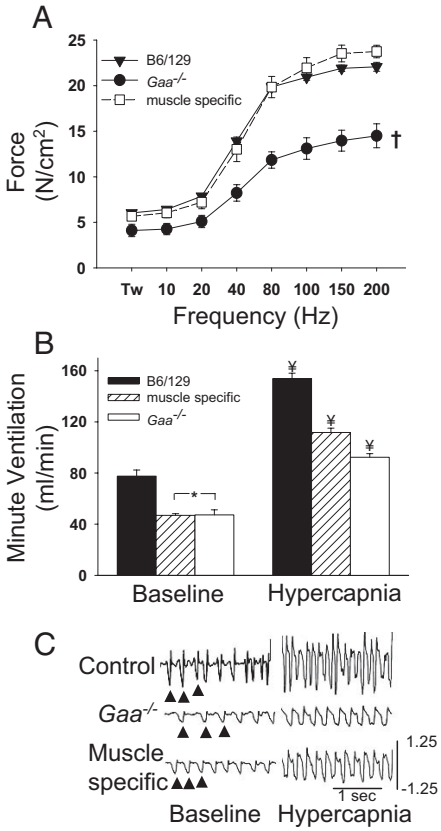

Fig. 3. Diaphragm contractility and ventilation in muscle-specific hGaa mice. (*A*) In vitro diaphragm contractility data for B6/129 (▼), $Gaa^{-/-}$ (●), and muscle-specific hGaa mice (□). Over a broad range of stimulation frequencies (Hz), the force developed by the muscle-specific hGaa diaphragm was similar to the B6/129 diaphragm (Tw = twitch force). Minute ventilation during baseline conditions was similar between muscle-specific and $Gaa^{-/-}$ mice (*B*). However, during a hypercapnic challenge (*B*), muscle-specific mice achieved ventilation that was greater than $Gaa^{-/-}$ mice but still less than B6/129 mice. Representative airflow tracings from unanesthetized mice during quiet breathing (baseline) and respiratory challenge (hypercapnia) are provided in *C* (arrows indicate breaths). The scaling is identical in all panels, and airflow calibration is in milliliters per second. *, Data are different from corresponding B6/129 data points; ¥, all groups are different from each other; †, $Gaa^{-/-}$ data are different from control and muscle-specific hGaa data ($P < 0.01$).

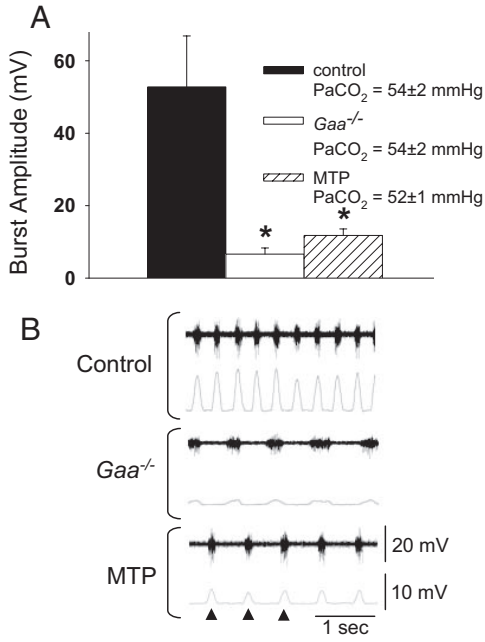

Fig. 4. Phrenic inspiratory burst amplitude recorded in anesthetized mice. The amplitude of the rectified and integrated phrenic inspiratory burst (see *Materials and Methods*) was quantified in control B6/129, $Gaa^{-/-}$, and muscle-specific hGaa mice during spontaneous breathing with similar arterial P_aCO_2 values (*A*). *, Different from control, $P < 0.01$. Typical examples of the unprocessed or "raw" phrenic neurogram (top traces) and the rectified, integrated neurogram (bottom traces) are shown in *B* (arrows indicate neural breaths). Scaling is identical between the 3 examples.

lines set forth by the Banbury Conference for studying genetically altered mice (22).

To obtain a comprehensive and complementary analysis of breathing in control and $Gaa^{-/-}$ mice, we combined plethysmography with phrenic neurophysiology, and both approaches point toward a similar conclusion. We show here, however, that the ventilatory responses in mice are reproducible despite the potential for technical caveats regarding the use of plethysmography (23, 24). The difference in body mass between control and $Gaa^{-/-}$ mice is another consideration. To account for the potential influence of body mass on ventilation data, an analysis of covariance was used (i.e., body mass as a covariate), and minute ventilation was also expressed relative to expired CO_2 (i.e., V_E/VCO_2 ratio) (Fig. S2).

Evidence for a Neural Contribution to Respiratory Deficits in $Gaa^{-/-}$ Mice. The reduced breathing frequency observed in both unanesthetized and anesthetized $Gaa^{-/-}$ mice may indicate a fundamental difference in the intrinsic activity of brainstem respiratory control neurons and/or networks in these mice compared with isogenic controls. Alternatively, a persistent change in chemoafferent and/or lung, airway, and chest wall afferent inputs could shape respiratory frequency in $Gaa^{-/-}$ mice. Arguing against a contribution of chemoafferent and/or vagally mediated signals is the observation that differences in phrenic burst frequency were observed between anesthetized and vagotomized $Gaa^{-/-}$ and control mice with comparable arterial blood gas values. Regardless of the mechanism, the reduced frequency may reflect a pathologic process that could not be offset by increased inspiratory volume. Indeed, the reduced breathing frequency was associated with a reduction in PaO_2.

The observation of excess glycogen within phrenic motoneurons (Fig. 1) coupled with increased phrenic soma size led us to compare inspiratory phrenic burst amplitude between control and $Gaa^{-/-}$ mice. Well-established electrophysiological techniques were used to measure compound action potentials (extracellular neurograms) in the phrenic nerve (25, 26). Both the phrenic burst amplitude associated with the initial onset of bursting after hypocapnia-induced apnea (control: 31.9 ± 0.3 mV; $Gaa^{-/-}$: 3.7 ± 0.9 mV) and during a hypercapnic challenge (control: 68.7 ± 20.0 mV; $Gaa^{-/-}$: 14.0 ± 4.8 mV) were apparently attenuated in $Gaa^{-/-}$ mice. Normalizations of phrenic inspiratory burst amplitude to a maximum (i.e., during gasping) and/or minimum (i.e., after apnea) value

Table 3. Phrenic neurophysiology characteristics

Group	Rate of rise, mV/sec	Frequency, breaths per minute	Amplitude, mV
Control	346 ± 86	167 ± 14	52.8 ± 14.1
$Gaa^{-/-}$	44 ± 15*	107 ± 14*	6.6 ± 1.7*
MTP	101 ± 27*	124 ± 17*	11.8 ± 1.8*

Rate of rise for the phrenic burst (mV/sec), frequency of the phrenic burst (neural breaths per second), and amplitude of the phrenic burst (mV) for 12-month-old control ($n = 8$), $Gaa^{-/-}$ ($n = 8$) and MTP ($n = 6$) mice.
*Different from control ($P < 0.01$).

are commonly performed under similar recording conditions (25, 26). The rationale for such normalizations, however, assumes that the ability to recruit phrenic motoneurons is not impaired (27). Accordingly, here we elected to simply present the raw data as one component of a comprehensive analyses of breathing in $Gaa^{-/-}$ mice. Taken together, the reduced respiratory frequency in both unanesthetized and anesthetized mice, and the apparently reduced phrenic nerve burst amplitude in anesthetized mice suggest a neural contribution to the deficits in ventilation observed in $Gaa^{-/-}$ mice.

The larger phrenic cell bodies observed in $Gaa^{-/-}$ mice and the large, swollen appearance of ventral horn cells in Pompe disease (refs. 9, 10, and 12, and the current study) may provide insight into one potential neural mechanism of impaired breathing associated with CNS GAA deficiency. According to Henneman's size principle, larger motoneurons require greater excitatory synaptic input for depolarization to occur than smaller motoneurons (28). Therefore, it is possible that the probability of phrenic motoneuron depolarization is lower in $Gaa^{-/-}$ mice and individuals with Pompe disease. The mechanisms responsible for the apparently reduced phrenic motoneuron recruitment in $Gaa^{-/-}$ mice likely also stem from areas beyond phrenic motoneurons, which include higher (neural) respiratory inputs and/or chemosensory afferents. Consistent with this suggestion, a recent report (3) described elevated glycogen in the $Gaa^{-/-}$ mouse ventral medulla. Another possibility is that $Gaa^{-/-}$ mice have altered sensory afferent input via respiratory or other peripheral nerves. Activation of phrenic (29), intercostal (30), and abdominal afferents (31) can all alter respiratory motor output (see also discussion in ref. 32). For example, activation of phrenic afferent neurons, including type I, III, and IV afferents, can inhibit phrenic motoneuron output (29). Increased activation of phrenic afferent pathways could impair diaphragm activity in $Gaa^{-/-}$ mice. The role of muscular afferents and segmental reflexes may be particularly important because Pompe patients have been shown to have fibrillation potentials in skeletal muscles (15). Moreover, Zellweger et al. (33) report markedly diminished (or absent) biceps, triceps, knee-jerk, and ankle-jerk reflexes in 2 Pompe infants. Absent or impaired reflexes also have been observed in other Pompe case reports (34–36).

In addition to excess glycogen within the CNS, the neural pathology suggested by these respiratory data also could be attributed to a lack of GAA activity during development, because GAA expression is highest in neural compared with all other immature tissues (37), and regulators of GAA are known to be necessary for CNS ontogeny and maturation (38).

Contribution of Diaphragm Muscle in Ventilation Deficits. To further test our hypothesis that muscular dysfunction is not the sole contributor to ventilation deficits associated with GAA deficiency, we used a double transgenic mouse that expressed hGAA only in skeletal muscle (maintained on the $Gaa^{-/-}$ background). Enzyme activity and hGAA gene expression in these mice have been described in detail (18). Because these mice had normal muscle contractile properties (Fig. 3A), we speculated that differences in ventilation between MTP and control strains would reflect a disparity in the neural control of respiratory muscles. The muscle-specific mice (MTP) had reduced ventilation during quiet breathing (baseline) that was similar to the full GAA knockout ($Gaa^{-/-}$) mice (Fig. 3*B*). When respiratory drive was stimulated with hypercapnia, the ventilatory response of MTP mice was still less than controls but was elevated compared with $Gaa^{-/-}$ mice (Fig. 3*B*). Contrasting the ventilation data obtained in MTP, $Gaa^{-/-}$, and control mice suggests that CNS GAA deficiency leads to inadequate neural drive to the respiratory muscles during quiet breathing conditions. During respiratory stimulation with hypercapnia, the higher ventilatory response in MTP vs. $Gaa^{-/-}$ mice suggests that both muscular and neural factors attenuate breathing in $Gaa^{-/-}$ mice. This conclusion is also supported by the neurophysiology data demonstrating attenuated respiratory frequency and apparently reduced phrenic burst amplitude in MTP mice.

Therapeutic Implications. Future studies of phrenic electrophysiology in humans with Pompe disease will be an important next step to understanding the causes of respiratory failure in this patient population. Indeed, our observations of substantially elevated glycogen and ventral cord neuronal pathology in the cervical spinal cord of a Pompe infant are consistent with the detailed $Gaa^{-/-}$ mouse data. However, as noted earlier, the $Gaa^{-/-}$ mouse may be a better model for late-onset Pompe disease, and neural respiratory deficits associated with early-onset Pompe disease could, in fact, be even greater. Consistent with this suggestion, the neuron pathology observed in the Pompe infant spinal cord was more advanced compared with the $Gaa^{-/-}$ mice (Fig. 1).

These findings have important implications for therapeutic strategies that will be effective in both the CNS and peripheral musculature. The current therapy for Pompe disease is enzyme replacement by i.v. delivery. However, the recombinant GAA enzyme does not cross the blood–brain barrier, where the protein may influence CNS GAA deficiency (17, 39). The results of enzyme replacement therapy have varied across the Pompe disease patient population (39–42), and detailed respiratory function data are still lacking in the early-onset patient population. Ongoing decline in ventilatory function as roughly measured by ventilatory failure has been observed in the first patient population to receive rhGAA therapy (43). We speculate that variability in respiratory function may reflect untreated CNS GAA deficiency that impairs the neural control of breathing. Because metabolically active motoneurons must function in the face of high demand or during fasting, small incremental changes in glycogen synthase activity in the absence of GAA activity leads to a more pronounced effect in these cells. The same cellular pathophysiology is evidenced by the effect of glycogen accumulation on the specialized conduction tissue in the heart.

The ability of new therapeutic options to reverse or lessen the degree of motor neuron dysfunction should be a focus of future investigations. Mechanical ventilatory support is currently in use but clearly is not a suitable lifelong solution. Consistent with other conditions of spinal cord injury, it may be appropriate to augment phrenic motor function by pacing. However, given the weakness in the extrathoracic musculature, phrenic pacing may prove to be difficult. Another possible approach could be respiratory rehabilitation strategies that promote plasticity in respiratory neurons and networks (44). Additional consideration is being given to approaches that either reduce the substrate for storage—a difficult task for glycogen—or provide a means of activating endogenous gene products via pharmacological chaperones. Although a limited number of mutations may be influenced by this approach, the potential for small molecules to improve respiratory function should be explored. Another means to restore GAA activity is the use of gene transfer, which has been studied in the context of respiratory dysfunction in Pompe disease (45). Clinical application of these therapeutic strategies alone or in combination with enzyme replacement therapy is a critical next step toward the successful management of Pompe disease.

Methods

Please see the *SI Methods* for additional methodological details.

Animals. The $Gaa^{-/-}$ and muscle-specific hGAA (MTP) mice have been described previously (18, 19). Contemporaneous sex-matched C57BL/6 × 129 × 1/SvJ mice were used as controls for all experiments. Mice were housed at the University of Florida specific pathogen-free animal facility. The University of Florida's Institutional Animal Care and Use Committee approved all animal procedures.

Glycogen Quantification and Histological Detection. Cervical spinal cord segments C_3–C_5 were harvested and stored at −80 °C until biochemical analysis of glycogen by using a modification to the acid-hydrolysis method (46). Spinal tissues were

also stained with PAS methods for histological glycogen detection by using the protocol of Guth and Watson (47).

Retrograde Phrenic Motoneuron Labeling. Fluorogold (4%; Fluorochrome) or CT-β (List Biological Laboratories) were applied to the peritoneal surface of the diaphragm, and 48 h later mice were anesthetized and the cervical spinal cord removed and sectioned. Fluorogold was identified by using fluorescence microscopy. CT-β was identified after incubation with antibody (goat anti-CT-β) by using light microscopy. We examined all labeled cells with a clear boundary and a visible nucleus.

Plethysmography. Plethysmography (Buxco) was used to quantify ventilation in male and female mice. Sexes were separated in the tables only when significant differences were detected (see *SI Methods*). A hypercapnic exposure (7% inspired CO_2) was used as a respiratory challenge as described previously (48). A subset of the current data was used as control data for a gene therapy intervention (45).

Arterial Blood Sampling. Arterial blood was analyzed with a commercially available system per the manufacturer's instructions (I-stat; Heska).

In Vitro Diaphragmatic Contractility. Mice were anesthetized, and the diaphragm was excised and placed into a dissecting chamber with Krebs–Henseleit solution equilibrated with a 95% O_2/5% CO_2 gas mixture. In vitro contractile measurements were performed as described previously (45).

Efferent Phrenic Nerve Recordings. Mice were anesthetized, tracheotomized, vagotomized, and mechanically ventilated. The right phrenic nerve was isolated by using a ventral approach, cut distally, and the proximal end placed on a bipolar tungsten wire electrode. Inspiratory phrenic electrical activity was then examined as described previously in rats (26).

Statistics. Statistical significance was set a priori at $P \leq 0.01$. Ventilation data were analyzed by using a 3-way analysis of covariance (ANCOVA). The ANCOVA method analyzed body weight as a covariate for respiratory volume data. For baseline measures, sex, strain, and age were used as factors, whereas the hypercapnic data were analyzed by using sex, strain, and time (minutes 1–10 of hypercapnia) as factors. Hb, Hct, glucose, and sodium (anesthetized mice) were analyzed by using the Student's *t* test. Glycogen quantification was analyzed by using a 2-way ANOVA and *t* test with Bonferroni correction for posthoc measurements. Diaphragmatic muscle contractile function was analyzed by using a 2-way ANOVA with repeated measures. Phrenic inspiratory burst amplitude, breathing frequency, and the rate of rise of the phrenic burst were extracted from the phrenic neurogram. These variables and arterial P_aO_2 were analyzed with the 1-way ANOVA and Fischer's LSD test for posthoc analysis. All data are presented as the mean $\pm$ SEM.

Pompe Infant Data. Autopsy permission was obtained by regular hospital procedures. Spinal cord and brain samples were either fixed in methanol or frozen in liquid N_2 rapidly upon autopsy and stored at -80 °C until assay. Glycogen was assayed by using magnetic resonance spectroscopy for natural abundance 13C and compared to a standard curve generated by using solutions with known glycogen content. For histological procedures, tissue was fixed and subsequently embedded in paraffin and sectioned at 7 μm. Tissues were stained with hematoxylin and eosin as well as PAS reagent.

ACKNOWLEDGMENTS. We thank Dr. Michael Lane, Dr. Sean Germain, Denise Cloutier, Stacy Porvasnik, and Sandy Walker for technical assistance. This work was funded by the National Institutes of Health Grants 1R01HD052682-01A1 (to D.D.F.), T32 HD043730 (to L.R.D.), HL59412 and DK58327 (to B.J.B.), and R01 NS054025-01 (to P.J.R.). L.R.D. was supported by the University of Florida Alumni Association Fellowship. K.C.D. was supported by the American Lung Association of Florida Research Training Fellowship.

1. Brown AM, Baltan Tekkök S, Ransom BR (2004) Energy transfer from astrocytes to axons: The role of CNS glycogen. *Neurochem Int* 45:529–536.
2. Vilchez D, et al. (2007) Mechanism suppressing glycogen synthesis in neurons and its demise in progressive myoclonus epilepsy. *Nat Neurosci* 10:1407–1413.
3. Sidman RL, et al. (2008) Temporal neuropathologic and behavioral phenotype of 6neo/6neo Pompe disease mice. *J Neuropathol Exp Neurol* 67:803–818.
4. Hirschhorn R, Reuser AJJ (2001) Glycogen storage disease type II; acid α-glucosidase (acid maltase) deficiency. In: *The Metabolic and Molecular Basis of Inherited Disease*, eds Scriver CR, Beaudet AL, Sly WS, Valle D (McGraw-Hill, New York), 8th Ed, Chapter 135.
5. Lejeune N, Thines-Sempoux D, Hers HG (1963) Tissue fractionation studies. 16. Intracellular distribution and properties of alpha-glucosidases in rat liver. *Biochem J* 86:16–21.
6. Jeffrey PL, Brown DH, Brown BI (1970) Studies of lysosomal alpha-glucosidase. I. Purification and properties of the rat liver enzyme *Biochemistry* 9:1403–1415.
7. Schoser B, Hill V, Raben N (2008) Therapeutic approaches in glycogen storage disease type II/Pompe Disease. *Neurotherapeutics* 5:569–578.
8. Raben N, Plotz P, Byrne BJ (2002) Correction of the enzymatic and functional deficits in a model of Pompe disease by using adeno-associated virus vectors. *Curr Mol Med* 2:145–166.
9. Teng YT, Su WJ, Hou JW, Huang SF (2004) Infantile-onset glycogen storage disease type II (Pompe disease): Report of a case with genetic diagnosis and pathological findings. *Chang Gung Med J* 27:379–384.
10. Mancall EL, Aponte GE, Berry RG (1965) Pompe's disease (diffuse glycogenosis) with neuronal storage. *J Neuropathol Exp Neurol* 24:85–96.
11. Martin JJ, de Barsy T, van Hoof F, Palladini G (1973) Pompe's disease: An inborn lysosomal disorder with storage of glycogen. A study of brain and striated muscle. *Acta Neuropathol (Berl)* 23:229–244.
12. Gambetti P, DiMauro S, Baker L (1971) Nervous system in Pompe's disease. Ultrastructure and biochemistry. *J Neuropathol Exp Neurol* 30:412–430.
13. Martini C, et al. (2001) Intractable fever and cortical neuronal glycogen storage in glycogenosis type 2. *Neurology* 57:906–908.
14. Chien YH, Lee NC, Peng SF, Hwu WL (2006) Brain development in infantile-onset Pompe disease treated by enzyme replacement therapy. *Pediatr Res* 60:349–352.
15. Hogan GR, Gutmann L, Schmidt R, Gilbert E (1969) Pompe's disease. *Neurology* 19:894–900.
16. Winkel LP, et al. (2005) The natural course of non-classic Pompe's disease; a review of 225 published cases. *J Neurol* 252:875–884.
17. Kikuchi T, et al. (1998) Clinical and metabolic correction of pompe disease by enzyme therapy in acid maltase-deficient quail. *J Clin Invest* 101:827–833.
18. Raben N, et al. (2001) Conditional tissue-specific expression of the acid alpha-glucosidase (GAA) gene in the GAA knockout mice: Implications for therapy. *Hum Mol Genet* 10:2039–2047.
19. Raben N, et al. (1998) Targeted disruption of the acid alpha-glucosidase gene in mice causes an illness with critical features of both infantile and adult human glycogen storage disease type II. *J Biol Chem* 273:19086–19092.
20. Seifert BL, et al. (1992) Development of obstruction to ventricular outflow and impairment of inflow in glycogen storage disease of the heart: Serial echocardiographic studies from birth to death at 6 months. *Am Heart J* 123:239–242.
21. Tankersley CG, Fitzgerald RS, Kleeberger SR (1994) Differential control of ventilation among inbred strains of mice. *Am J Physiol* 267:R1371–R1377.
22. Silva AJ, et al. (1997) Mutant mice and neuroscience: Recommendations concerning genetic background; Banbury conference on genetic background in mice. *Neuron* 19:755–759.
23. Enhorning G, van Schaik S, Lundgren C, Vargas I (1998) Whole-body plethysmography, does it measure tidal volume of small animals? *Can J Physiol Pharmacol* 76:945–951.
24. Mortola JP, Frappell PB (1998) On the barometric method for measurements of ventilation, and its use in small animals. *Can J Physiol Pharmacol* 76:937–944.
25. Baker TL, Mitchell GS (2000) Episodic but not continuous hypoxia elicits long-term facilitation of phrenic motor output in rats. *J Physiol* 529(Pt 1):215–219.
26. Fuller DD (2005) Episodic hypoxia induces long-term facilitation of neural drive to tongue protrudor and retractor muscles. *J Appl Physiol* 98:1761–1767.
27. Eldridge FL (1975) Relationship between respiratory nerve and muscle activity and muscle force output. *J Appl Physiol* 39:567–574.
28. Henneman E, Somjen G, Carpenter DO (1965) Functional significance of cell size in spinal motoneurons. *J Neurophysiol* 28:560–580.
29. Road JD (1990) Phrenic afferents and ventilatory control. *Lung* 168:137–149.
30. Romaniuk JR, Supinski GS, DiMarco AF (1993) Reflex control of diaphragm activation by thoracic afferents. *J Appl Physiol* 75:63–69.
31. Iscoe S, Grélot L, Bianchi AL (1990) Responses of inspiratory neurons of the dorsal respiratory group to stimulation of expiratory muscle and vagal afferents. *Brain Res* 507:281–288.
32. Teng YD, et al. (2003) Serotonin 1A receptor agonists reverse respiratory abnormalities in spinal cord-injured rats. *J Neurosci* 23:4182–4189.
33. Zellweger H, Dark A, Abu-Haidar GA (1955) Glycogen disease of skeletal muscle; report of two cases and review of literature. *Pediatrics* 5:715–732.
34. Willemsen MA, Jira PE, Gabreels FJ, van der Ploeg AT, Smeitink JA (1998) Three hypotonic neonates with hypertrophic cardiomyopathy: Pompe's disease. *Ned Tijdschr Geneeskd* 142:1388–1392.
35. Teng YT, Su WJ, Hou JW, Huang SF (2004) Infantile-onset glycogen storage disease type II (Pompe disease): Report of a case with genetic diagnosis and pathological findings. *Chang Gung Med J* 27:379–384.
36. Clement DH, Godman GC (1950) Glycogen disease resembling mongolism, cretinism, and amytonia congenita; case report and review of literature. *J Pediatr* 36:11–30.
37. Ponce E, Witte DP, Hirschhorn R, Huie ML, Grabowski GA (1999) Murine acid alpha-glucosidase: Cell-specific mRNA differential expression during development and maturation. *Am J Pathol* 154:1089–1096.
38. Ohtsuka T, et al. (1999) Hes1 and Hes5 as notch effectors in mammalian neuronal differentiation. Hes1 and Hes5 as notch effectors in mammalian neuronal differentiation. *EMBO J* 18:2196–2207.
39. Raben N, et al. (2003) Enzyme replacement therapy in the mouse model of Pompe disease. *Mol Genet Metab* 80:159–169.
40. Van den Hout JM, et al. (2004) Long-term intravenous treatment of Pompe disease with recombinant human alpha-glucosidase from milk. *Pediatrics* 113:e448–e457.
41. Winkel LP, et al. (2004) Enzyme replacement therapy in late-onset Pompe's disease: A three-year follow-up. *Ann Neurol* 55:495–502.
42. van Capelle CI, et al. (2008) Eight years experience with enzyme replacement therapy in two children and one adult with Pompe disease. *Neuromuscul Disord* 18:447–452.
43. Beck M (2007) New therapeutic options for lysosomal storage disorders: Enzyme replacement, small molecules and gene therapy. *Hum Genet* 121:1–22.
44. Lane MA, Fuller DD, White TE, Reier PJ (2008) Respiratory neuroplasticity and cervical spinal cord injury: Translational perspectives. *Trends Neurosci* 31:538–547.
45. Mah C, et al. (2007) Physiological correction of Pompe disease by systemic delivery of adeno-associated virus serotype 1 vectors. *Mol Ther* 15:501–507.
46. Lo S, Russell JC, Taylor AW (1970) Determination of glycogen in small tissue samples. *J Appl Physiol* 28:234–236.
47. Guth L, Watson PK (1968) A correlated histochemical and quantitative study on cerebral glycogen after brain injury in the rat. *Exp Neurol* 22:590–602.
48. Teng YD, Mocchetti I, Taveira-DaSilva AM, Gillis RA, Wrathall JR (1999) Basic fibroblast growth factor increases long-term survival of spinal motor neurons and improves respiratory function after experimental spinal cord injury. *J Neurosci* 19:7037–7047.